^{23}Na-nuclear magnetic resonance study of ionophore-mediated cation exchange between two populations of liposomes

A. Reginald Waldeck and Philip W. Kuchel
Department of Biochemistry, The University of Sydney, Sydney, New South Wales 2006, Australia

ABSTRACT A model system to observe and investigate the transfer of Na^+ ions between different internal compartments in a suspension of liposomes was developed, and the exchange was followed by nuclear magnetic resonance spectroscopy. The experiments were performed under conditions of a Donnan equilibrium. Quantitative analysis of this *three-site transmembrane* exchange system allowed us to distinguish between direct and indirect exchange between liposomes. It also disclosed a "confining" effect on the exchange between the two populations of liposomes. This confining effect may have been due to an electrostatic field in the presence of a membrane potential. Donnan potentials and ionic compositions at equilibrium for the three-compartment system were calculated numerically. The model system may be used to explore further the effects of membrane potentials, surface potentials, and ionic mobilities on ion transport in biological (model) systems in general.

INTRODUCTION

Vectorial ion transport and the maintenance of ionic gradients are essential to all living systems (1). There have been numerous studies on the maintenance and build-up of membrane potentials and pH gradients in cellular (2) and reconstituted systems (3, 4), as well as investigations into electrically silent phenomena (5). Physical phenomena, such as membrane surface potentials and unstirred layer (USL) effects, have been and still are extensively studied (6, 7). Theoretical studies of potential profiles in salt solutions bordered by a (biological) membrane, in the absence (8) and presence (9, 10) of a membrane potential, have been presented.

A number of physical phenomena exert an effect on solute concentrations in general, and ion concentrations in particular, in the vicinity of a (biological) membrane. First, in the presence of a membrane potential, one expects the electrical attractive forces acting on a cation and an anion to keep them in the vicinity of the membrane surface. On the other hand, both ions will tend to equilibrate with the adjacent bulk solutions. Second, surface potentials may significantly alter the "local" ion concentration at the membrane surface (6). Third, in the presence of a membrane impermeable ion, the permeable ions may redistribute so as to satisfy electroneutrality and equilibrium across the membrane, resulting in a Donnan equilibrium (11–13). Fourth, USL may cause the solute concentration adjacent to a membrane to differ from its bulk-solution value (7).

Nuclear magnetic resonance (NMR) is a useful tool for measuring the rate of transmembrane equilibrium exchange processes (14). A range of magnetization-transfer techniques have been successfully applied to the study of the transport of solutes, such as bicarbonate (15) and 3-fluoro-3-deoxy-D-glucose (16, 17) in human erythrocytes. Others have used NMR to monitor ionophore-mediated transmembrane exchange (18–20) and channel-mediated transport kinetics (21, 22) of various alkali-metal ions in model lipid vesicles.

In this study we aimed to verify whether solutes in general, and Na^+ ions in particular, are transported between *different* internal compartments in a suspension. To study this physical exchange, we chose a model system consisting of two populations of liposomes. We used the aqueous hyperfine shift reagents $DyPPP_2^{7-}$ and $TmPPP_2^{7-}$ (23, 24) and the ionophore M139603 (18) to set up a three-site physical exchange system, which may serve as a model of a cell suspension with two different populations of cells.

We observed qualitatively, and characterized quantitatively, the equilibrium exchange of Na^+ ions among the three sites. This was done using two-dimensional exchange spectroscopy (2D EXSY) (25–28), and one-dimensional "overdetermined" NMR exchange analysis (1D EXSY) (29), respectively. Experimental 2D EXSY spectra, together with theoretically predicted 2D EXSY spectra, allowed preliminary investigation into the possible factors involved in the transmembrane exchange of Na^+ ions in our system.

MATERIALS AND METHODS

Materials

L-α-phosphatidylcholine (PC) from fresh egg yolk was obtained from Sigma Chemical Co. (St. Louis, MO) as a chloroform solution. The ionophore M139603 (a Na^+/H^+-antiporter) was supplied by Pitman Moore Australia, Ltd. (Bringelly, NSW, Australia). D_2O was obtained from The Australian Institute for Nuclear Science and Technology (Lucas Heights, NSW, Australia). All other chemicals used were of analytical reagent grade. All solutions were prepared with reverse osmosis water and filtered through 0.2-μm cellulose acetate filters (Sar-

Address correspondence to Dr. Philip W. Kuchel, Department of Biochemistry, The University of Sydney, Sydney NSW 2006, Australia.

Part of this work was presented at the fifteenth annual meeting of the Australian Society for Biophysics in Sydney, NSW, Australia in December 1991.

torius GmbH, Göttingen, Germany) to remove any aggregates of paramagnetic ions. Cellulose acetate dialysis tubing, mol wt cutoff 12,000–14,000, was obtained from Spectrum Medical Industries Inc. (Los Angeles, CA). The shift reagents (SR) $DyPPP_2^{7-}$ and $TmPPP_2^{7-}$ were prepared from the lanthanide (III) chloride- and pentasodium tripolyphosphate complexes, in situ, as described previously (23). These SR induce a low- and high-frequency shift, respectively, to the NMR signals of the sodium ions with which they are in contact (23, 24). Standard polycarbonate membranes, used to filter and extrude the liposomes, were obtained from Poretics Co. (Livermore, CA). The bath sonicator used in the vesicle preparations was an ultrasonic cleaner (type B-220; Branson Cleaning Equipment Co., Shelton, CT).

Model system

Two populations of liposomes were prepared with different SR; one population contained ~4.7 mM $TmPPP_2^{7-}$, present in the external compartment only (Sample 1); the other population (Sample 2) contained 2.5 mM $DyPPP_2^{7-}$ within the liposomes, and the same concentration of $TmPPP_2^{7-}$ in the external medium (see Appendix 1B). "Fully relaxed" spectra of these samples are shown in Figs. 5 *A* and 4, respectively. Magnetization-transfer experiments were performed on these *two-site exchange* samples to evaluate the transmembrane influx and efflux rate constants. The two two-site exchange samples were then mixed to produce a *three-site exchange system,* comprised of two *different* internal—and one external—compartments (see Fig. 2).

The rationale behind performing NMR exchange experiments on not just a three-site exchange system, but also on each of the two-site exchange systems from which it was constructed, was to verify whether the experimentally observed amount of magnetization transferred between the *three* sites corresponded to that predicted from the amount of magnetization transfer that took place in the two *two*-site samples. A possible difference between the Na^+ concentration near the membrane surface and the bulk solution (see Fig. 1) might manifest itself in the magnitude of the cross-peaks in the 2D EXSY spectrum (see Fig. 3), which represent the amount of Na^+ exchange between the external and the two internal compartments (three-site exchange) during the "mixing time" of the experiment. To verify if such an effect was present or not, the experimental 2D EXSY spectrum was compared to a *simulated* 2D EXSY spectrum, which indicates the amount of Na^+ which has been exchanged among the three sites during the mixing time, *predicted* from the amount of magnetization transferred in the two two-site exchange systems. Conversely, a difference in the magnitude of the crosspeaks in the predicted and experimental 2D EXSY spectrum, representing transmembrane exchange, implies a difference in the values of particular exchange rate constants in the two- and three-site exchange samples.

Sample preparation

Solutions containing SR were prepared in a 1:2.5 lanthanide (III) to tripolyphosphate ratio, and were adjusted to pH 7.2. All solutions were adjusted to contain ~100 mM Na^+ (see Appendix 1B for exact compositions).

Large unilamellar vesicles (LUV) were made by the reverse-phase evaporation technique (30, 31). Briefly, 250 mg PC was dried down, as a thin lipid film, in a 250-ml round-bottom flask to which 24 ml diethylether, and subsequently 6 ml degassed buffer, was added. This mixture was bath-sonicated at ~4°C under argon until homogeneous; the process usually took ~15 min. The ether was then evaporated at reduced pressure at 30–35°C, until a semisolid gel was formed; this was vortexed and the organic phase was removed completely, resulting in a translucent aqueous suspension of liposomes. The suspension was filtered through a 3-μm polycarbonate membrane to remove any minor contamination of lipid aggregates. This method produces mainly uni- and some oligolamellar vesicles, with the bulk of the liposomes in the size range 200–500 nm in diameter (30, 31). Electron micrographs of a typical preparation revealed a predominantly unilamellar population of vesicles. The size range was estimated to be ~50–600 nm, with a rare structure exceeding 600 nm. LUV prepared without entrapped SR were stored overnight at 4°C. The suspension of LUV containing $DyPPP_2^{7-}$ was dialyzed overnight with one buffer change, against 2 liter of degassed buffer containing 95 mM NaCl and 5 mM NaP_i pH 7.2, while bubbled with nitrogen. Both suspensions were diluted 1:1 (vol/vol) in the $TmPPP_2^{7-}$ solution and left to equilibrate for 1 h at room temperature. The ionophore M139603 was added in a molar ratio to lipid of ~1:125, and the liposomes were collected by centrifugation at 30,000 *g* at 15–20°C for 1 h. For samples on which intrinsic T_1 experiments were performed, no ionophore was added to the suspensions. The percentage encapsulated aqueous volume was adjusted by addition of extraliposomal medium to the suspensions, and estimated by integrating the intra- and extraliposomal sodium resonances, as described previously (19, 21). These samples were used for NMR investigations.

Two similar experiments were run on 400- and 600-MHz NMR spectrometers tuned to ^{23}Na at 105.84 and 158.74 MHz, respectively. The higher frequency instrument was used to obtain better chemical shift dispersion. The samples run at 105.84 MHz (Figs. 3 and 4) were extruded through 0.6-μm polycarbonate membranes at 100 kPa under nitrogen at room temperature (after being filtered through a 3-μm membrane) to remove the largest liposomes. The samples run at 158.74 MHz (Fig. 5) were prepared as described above, except with half the amount of buffer, ether, and PC.

Experiments on the two-site exchange samples were carried out on a 1.5-ml suspension added to 10-mm NMR tubes for study at 105.84 MHz, or on 0.5-ml samples added to 5-mm NMR tubes for study at 158.74 MHz. The samples for study at 105.84 MHz were field-frequency locked on a 5-mm NMR tube containing pure D_2O. The samples run at 158.74 MHz were locked on 15% D_2O in the suspension. The three-site exchange sample run at 105.84 MHz was locked on a 2-mm o.d. coaxial capillary containing D_2O. All the samples were temperature equilibrated for at least 30 min before spectroscopic measurement. Temperature control on both spectrometers was better than ±1°C.

NMR methods

^{23}Na spectra were recorded on a wide-bore spectrometer (AMX 400; Bruker Instruments, Inc., Karlsruhe, Germany) and a spectrometer (AMX 600; Bruker Instruments, Inc.), both operating in the Fourier transform mode with quadrature detection. The 90° radio frequency pulse was 16–17 μs, using 4 dB attenuation at 158.74 MHz, for all experiments. The temperatures used are given in the figure legends.

Fully relaxed 1D spectra were acquired using 128 free induction decays (FID) with a repetition time of 150 ms ($\geq 5\ T_1$), covering a spectral width of 8,000 Hz using 1K datapoints. Spectral deconvolution was used to obtain the peak integrals in the spectrum obtained from the LUV *without* entrapped SR, run at 105.84 MHz.

1D EXSY experiments were performed using a standard Nuclear Overhauser Effect Spectroscopy (NOESY) pulse sequence (26, 29). Each spectrum was derived from 128 transients, of 1K datapoints over a spectral width of 8,000 Hz; the repetition time was 150 ms. The mixing times (t_m) used are given with Figs. 4 and 5. Peak integrals were determined from nonapodized spectra.

Longitudinal relaxation times (T_1) (Table 1) were measured using the composite-pulse T_1 program (32) and calculated using nonlinear least-squares regression (33) on a computer (model 9121; Hewlett-Packard Co., Palo Alto, CA). Sixteen delay times ranging from 50 μs to 300 ms or 50 μs to 400 ms were used to measure T_1 values in the presence of exchange and intrinsic T_1 values, respectively. Spectra were averaged over 128 transients.

Two-dimensional spectra (2D EXSY) were also obtained using the standard NOESY pulse sequence; $(t_w - \pi/2 - t_1 - \pi/2 - t_m - \pi/2 - t_2)_n$, with a repetition time greater than $4T_1$, and averaged over 512 transients. The acquisition parameters are given in the caption of Fig. 3. Cross-peak volumes were determined from a matrix of 512 × 512

TABLE 1 **Longitudinal relaxation times* in the absence and presence of exchange**

Site	Two Sites + Exchange		Three Sites − Exchange	Three Sites + Exchange
$Na_{in,1}^+$	28.0 ± 0.7		63.3 ± 1.9	29.3 ± 2.2
Na_{out}^+	22.7 ± 0.7‡	19.3 ± 0.3§	24.6 ± 0.8	21.3 ± 0.4
$Na_{in,2}^+$		19.2 ± 0.7	23.9 ± 0.4	23.6 ± 0.3

* T_1 ± SD (ms).
‡ T_1 of external Na^+ in LUV without entrapped SR.
§ T_1 of external Na^+ in LUV with entrapped SR($DyPPP_2^{7-}$).

datapoints, Fourier transformed after a shifted sinebell (SSB) apodization function (with $\theta = 90°$) in both time domains had been applied to the data.

BACKGROUND THEORY

The analysis of the 2D EXSY experiments (25–27) will be discussed here, as it is relevant to the prediction of the peak volumes of a simulated 2D EXSY spectrum represented in matrix form. The analysis of the 1D EXSY experiment is based on the 2D EXSY experiment and has been described elsewhere (29). The 2D EXSY spectrum may be viewed as the solution of the Bloch–McConnell differential equations, expressed in matrix form, that describe relaxation and magnetization exchange in a system. This solution is given by

$$\mathbf{A} = \exp-(\mathbf{R}t_m), \tag{1}$$

where **A** is the matrix of normalized 2D spectral peak volumes ($\mathbf{M}/\mathbf{M}_0$), consisting of **M**, whose elements are the peak volumes of the 2D EXSY spectrum, and $\mathbf{M}_0$, which is the diagonal matrix representing the 2D EXSY spectrum acquired with a mixing time (t_m) of zero seconds. **R** is the matrix of relaxation rate constants (in the diagonal elements) and the exchange rate constants (in the diagonal and off-diagonal elements), and has units (s^{-1}). In the case of a linear three-site exchange scheme, such as was shown to apply to the present system, the reactions are:

$$Na_{in,1}^+ \underset{k_{-1}}{\overset{k_1}{\rightleftharpoons}} Na_{out}^+ \underset{k_{-2}}{\overset{k_2}{\rightleftharpoons}} Na_{in,2}^+ \tag{2}$$

and **R** is given by:

$$\begin{bmatrix} 1/T_{1,in1} + k_1 & -k_{-1} & 0 \\ -k_1 & 1/T_{1,out} + k_{-1} + k_2 & -k_{-2} \\ 0 & -k_2 & 1/T_{1,in2} + k_{-2} \end{bmatrix}. \tag{3}$$

By backtransformation of matrix **A**, matrix **R** is found, and it contains the values of the exchange rate constants in the off-diagonal elements (25, 27):

$$\mathbf{R} = -1/t_m \ln \mathbf{A} = -1/t_m \mathbf{U}(\ln \Lambda)\mathbf{U}^{-1} \tag{4}$$

where Λ is a diagonal eigenvalue matrix; **U** and $\mathbf{U}^{-1}$ are the associated eigenvector matrices, such that $\mathbf{UAU}^{-1} = \Lambda$; Λ has diagonal elements (λ_i); and $\ln \Lambda = \text{diag}(\ln \lambda_i)$. We chose to quantitatively analyze our data using the 1D equivalent (1D EXSY) of this analysis, because of the relatively small cross-peak intensities in the 2D EXSY spectra. Also, because of the "overdetermined" nature of the experiment, greater accuracy is obtained in estimates of the values of the unitary rate constants per se (29).

Simulation of 2D EXSY spectra

Simulated 2D EXSY spectra were obtained by transformation of a matrix of exchange- and relaxation-rate constants, resulting in a NOESY matrix (**A**) of peak volumes:

$$\mathbf{A} = \exp-(\mathbf{R}t_m) = \mathbf{U}(\exp\Lambda)\mathbf{U}^{-1}, \tag{5}$$

where all symbols have the same meaning as mentioned above. Λ now has diagonal elements $-(\lambda_i t_m)$. The leading diagonal of the NOESY matrix ran from top left to bottom right as in the standard representation of a matrix, but this was converted to a 2D EXSY "spectrum" (as shown in Fig. 3), which conventionally runs from bottom left to top right.

The exchange matrix (**R**) was set up using the values for the exchange-rate constants obtained from 1D EXSY experiments, on the two-site exchange samples, together with intrinsic T_1 values obtained from T_1 experiments on a *different* three-site exchange sample *without* the ion carrier incorporated into the membranes. The format of matrix (**R**) was as given in Eq. 3; k_3 and k_{-3} (see Fig. 6) were assigned the value zero. The mixing time (t_m) entered in the simulation program was the one used in the 2D EXSY experiment. $\mathbf{M}_0$ was entered as a diagonal matrix of mole ratios obtained from a fully relaxed 1D spectrum (27).

Numerical procedures

1D EXSY and 2D EXSY data were analyzed on a computer (27, 29) (model 9121; Hewlett-Packard Co.). Deconvolution of equilibrium magnetization spectra was carried out with standard software (uxnmr version 911101.2; Bruker Instruments, Inc.).

Ionic compositions at equilibrium of each of the three compartments in the suspension of LUV were evaluated using the software package Mathematica on an Apple MacIntosh FX computer. The implicit quadratic expression obtained (see Appendix 1A) was solved using the command FindRoot (34).

RESULTS

Exchange model

Fig. 1 depicts the model of the three-site physical equilibrium exchange system that was postulated to apply to the transfer of sodium ions between two different populations of liposomes. Note that in reality the unitary first-

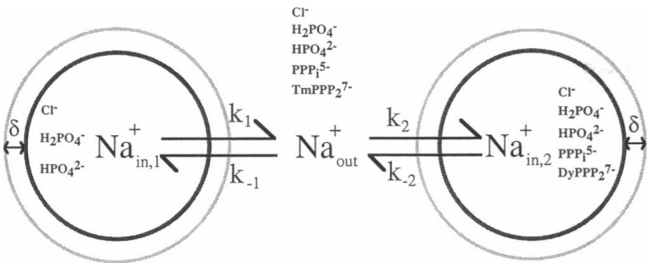

FIGURE 1 Schematic representation of the ionophore-mediated equilibrium exchange of sodium ions between different internal compartments in a suspension of two populations of liposomes, containing NaCl, NaP_i, Na_5PPP_i, Na_7DyPPP_2, and Na_7TmPPP_2. δ represents a USL or "screening" of the membrane by sodium ions, causing the sodium ion concentration adjacent to the membrane surface to differ from its value in the "bulk" solution. An internal layer δ may also exist, but it was omitted in the interest of clarity. $Na_{in,1}^+$ and $Na_{in,2}^+$ denote sodium ions within the encapsulated aqueous volume of each of the two liposome populations; Na_{out}^+ denotes sodium ions in the external medium. The k_i are unitary rate constants that characterize the exchange processes, and $DyPPP_2^{7-}$ and $TmPPP_2^{7-}$ are the reagents that shift the ^{23}Na NMR signal of Na^+ to low and high frequency, respectively.

order rate constants are in fact composite rate constants composed of a formation constant (k_f), a diffusion constant (k_{diff}), and a dissociation constant (k_d) (18, 35). Dynamic linebroadening due to transmembrane exchange is evident in Fig. 2, as was also observed in the two-compartment systems (18, 19, 22). This result suggested that it would be possible to observe the transfer of magnetization between the NMR signals corresponding to sodium nuclei in the internal and external compartments in a magnetization-transfer experiment. In fact, the overall exchange was rapid enough to observe magnetization being transferred from the sodium nuclei encapsulated in one of the populations of LUV, via the external medium, to the other population of LUV. Note in Fig. 2, that the high- (out) and low-frequency (in,2) $^{23}Na^+$ NMR resonances were broadened relative to the center resonance (in,1). The low-frequency $^{23}Na^+$ NMR resonance corresponding to sodium ions encapsulated by liposomes with entrapped $DyPPP_2^{7-}$ was broader than the high-frequency resonance corresponding to sodium ions in the external medium, even though the concentration of SR ($TmPPP_2^{7-}$) was higher in the latter; this difference was presumably caused by variations in the extent of entrapment of solutes by the LUV. Bulk magnetic susceptibility differences between compartments would have been present in the system due to the different concentrations of the (different) paramagnetic SR in the three compartments, and would have led to (differential) line-broadening (36, 37).

Verification of exchange between two internal compartments in suspensions of LUV

2D EXSY elegantly identifies multisolute chemical exchange networks by the presence of off-diagonal peaks between the exchanging partners (25–28). It has also been used to demonstrate transmembrane cation transport in two-site physical exchange systems (19, 21). Fig. 3 provides unequivocal evidence for Na^+-exchange between the two populations of LUV, by showing cross-peaks not only between the external and each of the internal magnetic environments, but also between each of the "internal" sodium resonances themselves. This was observed in a total of six samples prepared on separate occasions, in a similar manner. A control experiment on the same system, without ionophore incorporated into the membranes, did not exhibit crosspeaks between any of the resonances. A 2D EXSY experiment, performed under conditions virtually identical to those shown in Fig. 3, showed no cross-peaks between the two internal $^{23}Na^+$ resonances when the mixing time was decreased to 2 ms (cf. 6.5 ms). Cross-peaks between the external $^{23}Na^+$ resonance and each of the internal resonances were still evident (results not shown).

Kinetic characterization of the exchange system

Experimental determination of the unitary rate constants that characterize the exchange processes was carried out by means of 1D EXSY experiments, such as shown in Figs. 4 and 5. Fig. 4 shows the 1D EXSY experiment performed on one of the two-site exchange samples (extruded LUV), which was then used to obtain the 2D EXSY spectrum depicted in Fig. 3. Analysis of the spectra in Fig. 4, and of the other two-site exchange sam-

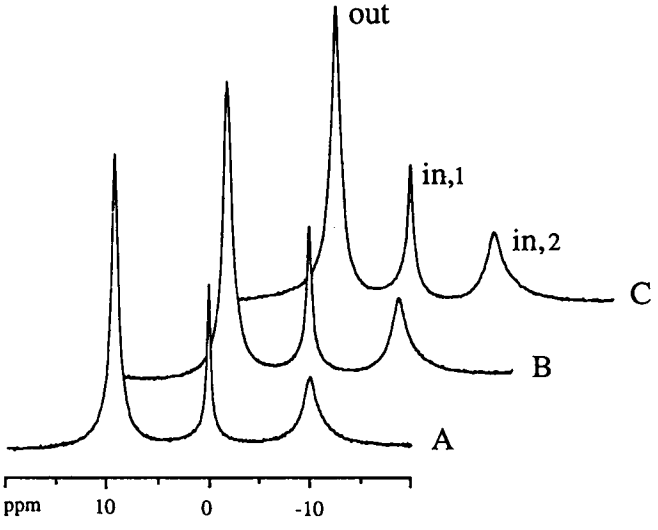

FIGURE 2 105.84 MHz ^{23}Na NMR spectra of a suspension of LUV containing two different internal compartments with the ionophore M139603 incorporated into the membranes at the different temperatures: *A*, 298K; *B*, 308K; *C*, 313K. The percentage encapsulated aqueous volume of each of the internal compartments was ~20%. Dynamic linebroadening was caused by the increase in transmembrane exchange rate with increasing temperature. A linebroadening factor of 5 Hz was applied to all fully relaxed spectra.

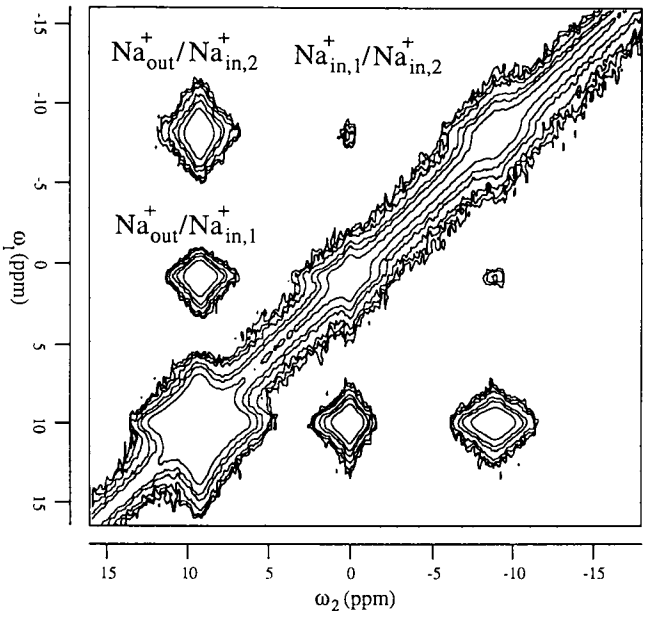

FIGURE 3 Contour plot from a 105.84 MHz ^{23}Na NMR 2D EXSY experiment on a suspension of liposomes containing two different internal compartments under equilibrium exchange conditions at 308 K. LUV with entrapped $DyPPP_2^{7-}$, which made up half of the sample, were the same as used for Fig. 4. The percentage encapsulated aqueous volume of each of the LUV was ~15%. The acquisition parameters for the 2D EXSY spectrum were: t_w = 79 ms; t_1 = 100 μs to 12.8 ms; t_m = 6.5 ms; t_2 = 51.2 ms; and n = 512. The spectral width was 6,000 Hz, with 512 datapoints. An SSB apodization function (with $\theta = 90°$) was used on the summed FID in both frequency domains prior to Fourier transformation. Other NMR parameters and procedures are as given in Materials and Methods.

ple (without entrapped $DyPPP_2^{7-}$), yielded the rate constant values (s^{-1}) $k_1 = 129.9 \pm 0.4$, $k_{-1} = 55.2 \pm 0.1$, $k_2 = 49.2 \pm 0.1$, and $k_2 = 97.4 \pm 0.3$; the errors were calculated as described previously (29). There was some degree of spectral overlap between the resonances from the "internal" sodium that was not in contact with SR and that of the "external" sodium; this overlap might have led to an erroneous result. However, a value of 1.06 for the ratio of the rates of flux in each direction, when in reality it must be 1.00, was deemed to be satisfactory.

To circumvent the problem of spectral overlap, the same experiments were carried out on similar (nonextruded) samples using the 600 MHz spectrometer (see Materials and Methods). The two-site exchange sample, without entrapped $DyPPP_2^{7-}$, and the three-site exchange sample yielded the spectra depicted in Fig. 5, *A* and *B*, respectively. The exchange-rate constants obtained from these experiments are given in Table 2.

Analysis of the 1D EXSY spectra shown in Fig. 5 *B* produced the exchange matrix (**R**) in Fig. 6 *B*. The corresponding putative exchange scheme is given in Fig. 6 *A*. Matrix **R** is of the same form as given in Eq. 3, but with non-zero values for k_3 (*top right*) and k_{-3} (*bottom left*), which suggests *direct* exchange between the two populations of LUV, as depicted in the cyclic model given in Fig. 6 *A*. However, these non-zero values most probably originate from "noise" generated in the analysis, and we took them to be not significantly different from zero because of their low values and relatively large standard deviations. Values of the order of 1 s^{-1} are below the expected sensitivity (detectibility) of the method, when the T_1 values are of the order of 10 ms.

Experimental and simulated 2D EXSY spectra

Although any apodization function may influence the values of peak integrals, it was found that an SSB function had a negligible effect on these values, compared with peak integrals of the same 2D EXSY spectrum determined with no apodization. This is because an SSB can be made to match the T_2 decay quite closely. Therefore an SSB (with $\theta = 90°$) apodization was used prior to Fourier transformation, because of the superior signal-

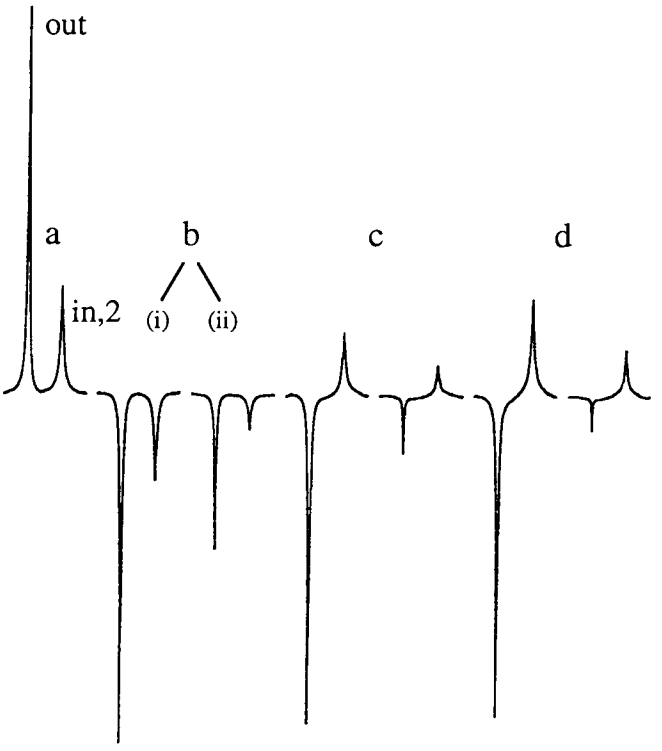

FIGURE 4 7 of the 17 ^{23}Na 105.84 MHz NMR spectra obtained from the overdetermined 1D EXSY of extruded LUV with entrapped $DyPPP_2^{7-}$. An exponential multiplication factor of 15 Hz was applied to the FID prior to Fourier transformation. The fully relaxed equilibrium magnetization spectrum is *a*. The percentage encapsulated aqueous volume was ~30%. Spectra *b*–*d* are 1D EXSY experiments (see Materials and Methods). Spectra (*i*) and (*ii*) were obtained using mixing times of 0 and 5 ms, respectively. The evolution times used in this experiment varied from 3 μs in steps of 1/8 to 7/8 × (3/4$\Delta\nu$), where $\Delta\nu$ was the chemical shift difference (in Hz) between the extra- and intraliposomal resonances, from species in direct contact with $DyPPP_2^{7-}$. The evolution times for spectra *b*, *c*, and *d* were 3, 240.4, and 336.5 μs, respectively.

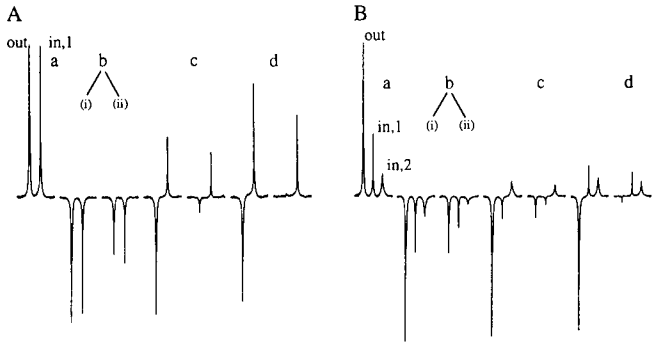

FIGURE 5 7 of the 17 ^{23}Na NMR 1D EXSY spectra acquired at 158.74 MHz at 311 K. A line-broadening factor of 10 Hz was applied to all spectra. (*A*) Two-site exchange sample without entrapped SR. The linewidths for the intra- and extraliposomal resonances were 69 and 126 Hz, respectively, and the chemical shift separation ($\Delta\nu$) was 9.45 ppm. The equilibrium magnetization spectrum is *a*. The percentage encapsulated aqueous volume was ~40%. Spectra (*i*) and (*ii*) were obtained using mixing times of 0 and 6 ms, respectively. The evolution times used in this experiment varied from 3 μs in steps of $\frac{1}{8}\times$ to $\frac{7}{8}\times(\frac{3}{4}\Delta\nu)$. The evolution times for spectra *b*, *c*, and *d* were 3, 187.5, and 375.0 μs, respectively. (*B*) Three-site exchange sample. The linewidths of the external sodium resonance, internal sodium resonance without entrapped SR, and internal sodium resonance with entrapped SR were 122, 73, and 240 Hz, respectively; the chemical shift separation between the two internal sodium resonances was 8.73 ppm; and the separation between the external and internal sodium resonance with entrapped SR was 17.81 ppm. The equilibrium magnetization spectrum is *a*. The percentage encapsulated aqueous volume of each of the LUV samples was ~20%. Spectra (*i*) and (*ii*) were obtained using mixing times of 0 and 6.5 ms, respectively. The evolution times used in this experiment varied from 3 μs in steps of $\frac{1}{8}$ to $\frac{7}{8}\times(\frac{3}{4}\Delta\nu)$. The evolution times for spectra *b*, *c*, and *d* were 3, 99.6, and 199.2 μs, respectively.

to-noise ratio that emerged in the spectra. The peak volumes of the experimental 2D EXSY spectrum (run at 158.74 MHz) are given in Fig. 7 *A*. Note that the diagonal elements (*lower left* to *upper right*) do not accurately describe the percentage encapsulated aqueous volume of the relevant compartments. This was caused by the spectral overlap of the large "wings" of the $^{23}Na^+$ resonances in the diagonal of the spectrum.

The peak volumes of the simulated 2D EXSY spectrum are shown in Fig. 7 *B*. Peak volumes of both the experimental and the predicted NOESY spectrum were normalized to give the lower left-hand peak (Na_{out}^+) the value 10.00. Although the simulated 2D EXSY spectrum in Fig. 7 *B* appears "unbalanced" (asymmetrical), it is clear that the cross-peak intensities are greater, relative to the diagonal peak intensities, when compared with the experimental 2D EXSY spectrum (Fig. 7 *A*). The unbalanced nature of the simulated 2D EXSY spectrum was caused by the sensitivity to the input data of the analysis in the simulation program; it became more balanced when k_3 and k_{-3} were given the values of 7.2 (s^{-1}) and 4.4 (s^{-1}), respectively, that were obtained from the corresponding 1D EXSY analysis.

DISCUSSION

In cell suspensions, an intracellular solute, which is transported across the membrane of one cell, is expected to enter another cell by means of diffusion through the extracellular medium. It may be translocated into the other cell via a transport protein or channel. It was sodium ion transport under equilibrium exchange conditions, between two populations of internal compartments in a suspension of liposomes, that we aimed to "visualize" experimentally. In this study we showed that:

(*a*) The exchange of sodium ions between two different populations of liposomes can be monitored by NMR. Any possible degradation of the sample during the experiment was checked by measuring the linewidths, chemical shifts, and integrals of the acquired spectra, before and after the experiments. The 2D EXSY spectra (e.g., Fig. 3) were acquired in ~170 min. The chemical shift of each of the three $^{23}Na^+$ resonances varied by no more than 6 Hz, and the linewidths by no more than 3 Hz at either 105.84 or 158.74 MHz. The peak integral values remained constant. Net sodium transport during the timecourse of the experiment, release of SR from the vesicles, and/or vesicle fusion, would be expected to have altered the chemical shifts and linewidths. Therefore, the system was taken to be at equilibrium and stable during the experiments. The LUV were prepared at pH 7.2 instead of pH 8.0–8.1 as in previous studies (18–22, 35). The homogeneous entrapment of SR was found not to be reproducible at pH 8.0, but it was at the lower pH. Protons interact with phospholipid headgroups (38), and therefore this interaction may affect the homogeneous entrapment of SR.

A potential problem with the analysis of the data obtained from the vesicles is that the "internal" Na^+ ions could be trapped between lamellae of a small fraction of multilamellar vesicles; LUV prepared by the reverse-phase evaporation technique routinely contain ~90%

TABLE 2 Exchange rate constants in two-site and three-site exchange systems*

(s^{-1})	k_1	k_{-1}	k_2	k_{-2}	k_3	k_{-3}
two-site‡	100.9 ± 0.2	56.6 ± 0.1	80.7 ± 0.1	111.4 ± 0.3		
three-site§	95.7 ± 0.8	25.3 ± 0.1	22.7 ± 0.1	92.0 ± 0.5	7.2 ± 0.6	4.4 ± 0.9

* Determined using the 1D "overdetermined" exchange analysis (1D EXSY).
‡ Parts of the scheme of Fig. 1.
§ The whole scheme of Fig. 1.

A

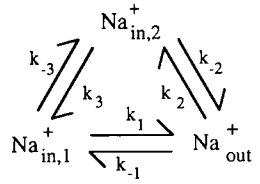

B

$$\begin{bmatrix} 123.3 & -25.3 & -7.2 \\ -95.7 & 110.4 & -92.0 \\ -4.4 & -22.7 & 124.6 \end{bmatrix}$$

FIGURE 6 (*A*) Cyclic three-site scheme for the equilibrium exchange of sodium ions between two internal compartments in a suspension of LUV. (*B*) Exchange matrix **R** obtained from the data shown in Fig. 5 *B*.

unilamellar vesicles (30). In the former case, the cross-peaks between the "internal" sodium resonances in the 2D EXSY spectrum (Fig. 3) could have arisen from the exchange of Na^+ ions, which were in contact with SR encapsulated by one lamella, and Na^+ ions not in contact with SR, encapsulated by an adjacent lamella of the *same* multilamellar vesicle. However, preliminary experiments using frozen and thawed multilamellar vesicles (FATMLV) (39), resulted in spectra with a very broad and asymmetrical "internal" $^{23}Na^+$ NMR resonance, when the SR was added between freeze and thaw cycles (results not shown). In this procedure, at least part of the entrapped SR was probably present in the aqueous volume between lamellae of the putative multilamellar vesicles.

(*b*) *Direct* exchange of sodium ions between two LUV, as depicted in the scheme in Fig. 7 *A*, did not occur to any significant extent, as evidenced by the very low estimates of k_3 and k_{-3} in the kinetic matrix (Fig. 6 *B*). Direct exchange might have been caused by exchange of an ionophore–sodium *complex* between vesicles; the sodium ion would then not become solvated by the water molecules in the bulk phase, but would be transported through two consecutive bilayers of adjacent vesicles. Since diffusion through the lipid bilayer (k_{diff}) was found not to be the rate-limiting step in the "overall" transmembrane exchange of ion carriers, such as M139603 (18), and monensin (20), this direct exchange between two LUV, if it occurs, should also be rapid. Therefore we concluded that a significant amount of slow transport was unlikely. Although direct exchange of Na^+ ions between adjacent liposomes was not manifest in the present systems, with a combined percentage encapsulated aqueous volume of both internal magnetic environments of 30–40%, it is possible that this could take place with a higher packing density.

(*c*) The discrepancy between the experimental (Fig. 7 *A*) and the simulated (Fig. 7 *B*) data suggests that there is a physical phenomenon that leads to a reduced rate of exchange in the three-site site system, a phenomenon that does not manifest itself in each two-site system when studied separately. All the cross-peak intensities in the experimental 2D EXSY spectrum (Fig. 7 *A*) are of lesser intensity, relative to the corresponding diagonal peak intensities, than in the simulated 2D EXSY spectrum (Fig. 7 *B*). This implies lower values of the influx rate constants, k_{-1} and k_2 (see Table 2). Comparison of a NOESY matrix (2D EXSY spectrum) simulated from the exchange matrix in Fig. 6 *B* (obtained from 1D EXSY analysis at 158.74 MHz), with the simulated NOESY matrix in Fig. 7 *B*, demonstrated a similar trend. Simulated and experimental data from the experiments run at 105.84 MHz also showed a similar result. A possible explanation for the observed effect is that there is a USL (δ, in Fig. 1) and that in the two-site case ions pass into and out of this layer when exchanging across the membrane, with fewer actually entering the bulk phase.

Also, a Donnan equilibrium would have existed in the two- and three-site exchange systems, because of the presence of the membrane-impermeable SR and phosphate ions. At equilibrium, this non-permeability would have caused a higher Na^+, and a lower Cl^- concentration, in the compartment with SR or a relatively high concentration of SR (see Appendix 1B). No active ion-transport system was present in the vesicles, and since M139603 only exchanges cations, the (Donnan) equilibrium would not have changed over time. Peak integrals corresponding to each of the "internal" $^{23}Na^+$ resonances in the three-site sample were measured (within experimental error) to be half of their values in the corresponding two-site samples, which indicated that the combined percentage encapsulated aqueous volume remained essentially unchanged.

Note, however, that because of the Donnan equilibrium, the peak integrals are not an exact measure of the percentage encapsulated aqueous volume, as described previously (19, 21), because at equilibrium the sodium ion concentrations in the different compartments will no longer be the initial ones. This effect would not have been large in the present system (nor in previous studies), because the Donnan effect is essentially obscured by a high NaCl concentration (11) (see also Appendix

A

$$\begin{bmatrix} 0.66 & 0.07 & 1.95 \\ 1.06 & 2.84 & 0.08 \\ 10.00 & 1.10 & 0.81 \end{bmatrix}$$

B

$$\begin{bmatrix} 5.32 & 0.69 & 3.24 \\ 4.31 & 3.67 & 0.53 \\ 10.00 & 2.34 & 2.34 \end{bmatrix}$$

FIGURE 7 Matrices of normalized peak volumes of 2D EXSY spectra; the lower left-hand corner peak (Na_{out}^+) was set to the value 10.00. (*A*) Experimentally obtained matrix from the 2D EXSY spectrum obtained at 158.74 MHz (not shown) processed with an SSB function (with $\theta = 90°$) in both dimensions. (*B*) Simulated matrix obtained by transformation of the exchange matrix obtained from 1D EXSY experiments, e.g., Fig. 5 *A*, and measurements of the intrinsic T_1 values in the two-site exchange samples.

1B), but it does lead to a systematic overestimation of the relative volume of the compartment, corresponding to Na^+ ions in contact with the SR.

This redistribution of ions across the membrane results in a membrane potential, *negative outside* relative to inside, for each of the two-site systems and for the three-site system. Even in the presence of a small membrane potential of a few millivolts, as was the case for our system (see Appendix), the electrical field across the membrane, and therefore the coulombic force acting on a sodium ion, may be substantial. A *positive* Na^+ ion entering the external phase would be subject to electrostatic *repulsion,* which may retard its diffusion into the bulk phase.

This retardation, or reduced rate of ions entering the bulk phase, in the presence of a membrane potential has been observed previously (10, and references therein). When an electrical potential difference exists between solutions on either side of a membrane partition, a space charge layer is built up in the vicinity of the membrane (9). In their treatment of a membrane bordered by homogeneous salt solutions, Laüger et al. (9) showed that, in the presence of a membrane potential, a small number of ions would accumulate near the membrane within a layer of which the thickness approximates the "Debye–Hückel length." Kamp et al. (10) demonstrated that this effect, as observed for protons, could be explained by the effects of electrostatic fields in the presence of immobile proteins, which are abundant in energy-transducing membranes, and/or mobile buffers. Previous work has shown that screening of PC-bilayers by NaCl solutions is negligible (40), and therefore a surface potential could not have caused our observed effect. However, a high diffusional resistance for Na^+ ions in the putative USL, due to a high membrane permeability (7) for Na^+ in the presence of an ionophore, may also have been present.

In conclusion, this study is to our knowledge the first NMR demonstration of rapid exchange of a solute between internal compartments in a cell or vesicle suspension. Multisite *chemical* exchange systems have been characterized kinetically by NMR (25–28), but no study of a multisite *physical* exchange system has been reported previously. Completely resealing cells to low molecular weight solutes, such as SR, after permeabilization is troublesome (41); our attempts to entrap SR in human erythrocytes were unsuccessful. Therefore we chose to use lipsomes. Studies reporting the use of low- and high-frequency SR, in combination, and their use in three-compartment systems have been scarce (24, 42). Apart from the potential use in epithelial tissue, already mentioned by Chu et al. (24) in 1984, this study shows the relevance to artificial lipid bilayer systems. The present three-site exchange model may provide a means of further substantiating the "confining" effect by alteration of the Donnan potential. This may be done by variation of the relative concentrations of SR and/or use of non-chelating impermeant ions in each compartment. The present model system might also be extended to investigate the effect of a surface potential on the ionophore-mediated sodium and lithium exchange between two different populations of LUV containing phosphatidylserine (PS). Riddell and co-workers (18, 35) demonstrated a kinetic effect on the monensin-mediated lithium transport in PC/PS-liposomes at 5% PS loading (35). Thermodynamic effects, such as cation "screening" of and binding to PS-headgroups, operate in these experiments; lithium displays "hard" interactions with PS (35, 38). A decrease of the "lateral" diffusion coefficient (adjacent to a surface) of Li^+, and to some extent Na^+, was observed in anionic surfactant systems (43, 44). These effects can be expected to exert an effect on the exchange of these ions between two different populations of LUV containing negatively charged phospholipids. The effect of different ionic mobilities may be studied using the chloride salts of Na^+, Li^+, and Cs^+, since these nuclei all possess good NMR receptivity and vary considerably in ionic mobilities.

Finally, there appear to be many possible applications of the present three-site system in exploring factors that affect ion transport between liposomes and cells.

APPENDIX

1A. Donnan equilibrium in a three-compartment system

Only the derivation of the implicit quadratic expression, obtained by using the conditions of conservation of mass, electroneutrality, and equilibrium of permeable ions across the membrane, for a three-site system, is given here. For each of the *two*-site systems, the ionic compositions at equilibrium and the Donnan potentials were calculated using the conservation and equilibrium conditions (see below) relevant to two compartments, as described previously (11–13).

In these calculations we assumed a) that the LUV are rigid compartments; e.g., the peak integrals corresponding to "internal" Na^+ remained unchanged upon mixing (see Discussion); b) that we could ignore H^+ buffering of P_i, since P_i concentrations were low, and H^+ concentrations at equilibrium in the respective compartments would have remained negligible compared with the salt concentrations.

Permeant ions: Na^+ and Cl^-.

Impermeant ions: $HPO_4^{2-}(P_i^{2-})$, $HPO_4^{-}(P_i^{1-})$,

PPP_i^{5-}, $TmPPP_2^{7-}$, $DyPPP_2^{7-}$.

Conservation of mass for Na^+ and Cl^{-1} given in molar concentrations (the superscript m denotes moles):

$$Na_{total}^{+m} = Na_{in,1}^{+}V_{in,1} + Na_{out}^{+}V_{out} + Na_{in,2}^{+}V_{in,2} \quad (A1)$$

$$Cl_{total}^{-m} = Cl_{in,1}^{-}V_{in,1} + Cl_{out}^{-}V_{out} + Cl_{in,2}^{-}V_{in,2}. \quad (A2)$$

At equilibrium the free energy of the exchangeable ions is the same in each compartment, therefore:

$$Na_{in,1}^{+}Cl_{in,1}^{-} = Na_{out}^{+}Cl_{out}^{-} = Na_{in,2}^{+}Cl_{in,2}^{-}. \quad (A3)$$

Electroneutrality (at equilibrium) requires that:

$$Na_{in,1}^{+} = Cl_{in,1}^{-} + 2P_{i_{in,1}}^{2-} + P_{i_{in,1}}^{1-} \quad (A4)$$

$$Na_{out}^{+} = Cl_{out}^{-} + 2P_{i_{out}}^{2-} + P_{i_{out}}^{1-}$$

$$+ 5PPP_{i_{out}}^{5-} + 7TmPPP_{2_{i,out}}^{7-} \quad (A5)$$

$$Na_{in,2}^{+} = Cl_{in,2}^{-} + 2P_{i_{in,2}}^{2-} + P_{i_{in,2}}^{1-} + 5PPP_{i_{in,2}}^{5-} + 7DyPPP_{2_{in,2}}^{7-}. \quad (A6)$$

Using Eqs. A2, A4, and A5, we obtain for the first equality of Eq. A3:

$$(Cl_{in,1}^{-} + 2P_{i_{in,1}}^{2-} + P_{i_{in,1}}^{1-})Cl_{in,1}^{-} = \left(\frac{Cl_{total}^{-m}}{V_{out}} - \frac{Cl_{in,1}^{-}V_{in,1}}{V_{out}} - \frac{Cl_{in,2}^{-}V_{in,2}}{V_{out}}\right) \times \left(\frac{Cl_{total}^{-m}}{V_{out}} - \frac{Cl_{in,1}^{-}V_{in,1}}{V_{out}} - \frac{Cl_{in,2}^{-}V_{in,2}}{V_{out}} + 2P_{i_{out}}^{2-} + P_{i_{out}}^{1-} + 7TmPPP_{2_{out}}^{7-} + 5PPP_{i_{out}}^{5-}\right). \quad (A7)$$

We now define:

$$Cl_{in,1}^{-} = x;$$
$$Cl_{in,2}^{-} = y;$$
$$2P_{i_{in,1}}^{2-} + P_{i_{in,1}}^{1-} = a;$$
$$\frac{Cl_{total}^{-m}}{V_{out}} = b;$$
$$2P_{i_{out}}^{2-} + P_{i_{out}}^{1-} + 7TmPPP_{2_{out}}^{7-} + 5PPP_{i_{out}}^{5-} = c;$$
$$2P_{i_{out}}^{2-} + P_{i_{out}}^{1-} + 7DyPPP_{2_{out}}^{7-} + 5PPP_{i_{out}}^{5-} = d$$

and obtain:

$$(x + a)x = b^2 - \frac{V_{in,1}}{V_{out}}bx - \frac{V_{in,2}}{V_{out}}by - \frac{V_{in,1}}{V_{out}}bx + \left(\frac{V_{in,1}}{V_{out}}\right)^2 x^2 + \frac{V_{in,1}V_{in,2}}{V_{out}^2}xy - \frac{V_{in,2}}{V_{out}}by + \frac{V_{in,1}V_{in,2}}{V_{out}^2}xy + \left(\frac{V_{in,2}}{V_{out}}\right)^2 y^2 + bc - \frac{V_{in,1}}{V_{out}}cx - \frac{V_{in,2}}{V_{out}}cy. \quad (A8)$$

This is equal to:

$$x^2\left(1 - \left(\frac{V_{in,1}}{V_{out}}\right)^2\right) + x\left(a + 2\frac{V_{in,1}}{V_{out}}b - 2\frac{V_{in,1}V_{in,2}}{V_{out}^2}y + \frac{V_{in,1}}{V_{out}}c\right) + \left(2\frac{V_{in,2}}{V_{out}}by + \frac{V_{in,2}}{V_{out}}cy - b^2 - \left(\frac{V_{in,2}}{V_{out}}\right)^2 y^2 - bc\right) = 0. \quad (A9)$$

We define:

$$\left(1 - \left(\frac{V_{in,1}}{V_{out}}\right)^2\right) = A;$$
$$\left(a + 2\frac{V_{in,1}}{V_{out}}b - 2\frac{V_{in,1}V_{in,2}}{V_{out}^2}y + \frac{V_{in,1}}{V_{out}}c\right) = B;$$
$$\left(2\frac{V_{in,2}}{V_{out}}by + \frac{V_{in,2}}{V_{out}}cy - b^2 - \left(\frac{V_{in,2}}{V_{out}}\right)^2 y^2 - bc\right) = C.$$

The solution to the quadratic expression (Eq. A9) in x ($=Cl_{in,1}^{-}$) is:

$$x = \frac{-B + \sqrt{B^2 - 4AC}}{2A}. \quad (A10)$$

Substituting Eqs. A4 and A6 into Eq. A3 yields:

$$(Cl_{in,1}^{-} + a)Cl_{in,1}^{-} = (Cl_{in,2}^{-} + d)Cl_{in,2}^{-}. \quad (A11)$$

We thus obtain an (implicit) quadratic expression for $Cl_{in,2}^{-}$ in terms of $Cl_{in,1}^{-}$:

$$(\lambda + a)\lambda - Cl_{in,2}^{-2} - Cl_{in,2}^{-}d = 0 \quad \text{with} \quad x = \lambda \equiv \lambda(Cl_{in,2}^{-}). \quad (A12)$$

$Cl_{in,2}^{-}$ was obtained by numerically solving Eq. A12 for its real positive root; for this we used Mathematica (34). Having obtained $Cl_{in,2}^{-}$, we then obtained $Cl_{in,1}^{-}$ from Eq. A10, $Na_{in,1}^{+}$ from Eq. A4, $Na_{in,2}^{+}$ from Eq. A6, Na_{out}^{+} from Eq. A1, and Cl_{out}^{-} from Eq. A3.

1B. Results

Donnan ratios, Donnan potentials, and ionic compositions at equilibrium

LUV were prepared at ~42 mg/ml lipid, which resulted in a percentage encapsulated aqueous volume of ~30%, as estimated from the $^{23}Na^{+}$ spectral integrals of an LUV sample that was not concentrated by centrifugation. The samples, which were extruded through 0.6-μm membranes, demonstrated a similar percentage encapsulated aqueous volume. Therefore, in the calculations the (initial) fractional internal and external volumes were taken to be 0.3 V_{total} and 0.7 V_{total}, respectively, and the suspensions were always mixed in a 1:1 (vol/vol) ratio. The solution compositions at equilibrium are valid for the samples run at 105.84 and 158.74 MHz. LUV were mixed, but not *diluted*, at the greater percentage encapsulated aqueous volume ($V_{in} = 0.4V_{total}$; 158.74 MHz samples). The preequilibrium solution composition of the LUV with entrapped $DyPPP_2^{7-}$ (Sample 2) after dialysis was taken to be the "IN1" solution composition, and the "final" Donnan equilibrium for this sample was calculated after the dilution of this sample, with its solution composition determined by the "initial" Donnan equilibrium (after dialysis), into external (OUT) solution. The Donnan potentials given here were calculated for T = 308 K (105.84 MHz); potentials at 311 K (158.74 MHz) were identical within one significant figure.

——1/Original suspension media used in the preparation of LUV and dilution of suspensions of LUV:

Ion	IN 1	OUT	IN 2
Na^+	104.50	100.0	102.025
Cl^-	95.45	24.0	73.75
$H_2PO_4^-$	0.95		0.475
HPO_4^{2-}	4.05		2.025
PPP_i^{5-}		4.0	1.25
$DyPPP_2^{7-}$			2.5
$TmPPP_2^{7-}$		8.0	

——2/Sample 1, two-site system: $TmPPP_2^{7-}$ present externally only; system at equilibrium.

Ion	IN 1	OUT 1	r_{Donnan}	V_m, mV
Na^+	86.67	109.64	1.265	6.3
Cl^-	77.62	61.51		
$H_2PO_4^-$	0.95	0.39		
HPO_4^{2-}	4.05	1.67		
PPP_i^{5-}		2.3		
$DyPPP_2^{7-}$				
$TmPPP_2^{7-}$		4.700		

——3/Sample 2, two-site system: $DyPPP_2^{7-}$ present internally, and $TmPPP_2^{7-}$ present externally; system at equilibrium.

Ion	IN 2	OUT 2	r_{Donnan}	V_m, mV
Na^+	94.775	107.21	1.131	3.3
Cl^-	66.5	58.83		
$H_2PO_4^-$	0.475	0.39		
HPO_4^{2-}	2.025	1.67		
PPP_i^{5-}	1.25	2.35		
$DyPPP_2^{7-}$	2.5			
$TmPPP_2^{7-}$		4.7		

——4/Three-site system: system at equilibrium; composition calculated using the theory in Appendix 1A.

Ion	IN 1	OUT	IN 2	$r_{Donnan,1}$	$r_{Donnan,2}$	$V_{m,1}$, mV	$V_{m,2}$, mV
Na^+	85.405	108.408	96.119	1.269	1.128	6.3	3.2
Cl^-	76.355	60.153	67.844				
$H_2PO_4^-$	0.95	0.39	0.475				
HPO_4^{2-}	4.05	1.67	2.025				
PPP_i^{5-}		2.325	1.25				
$DyPPP_2^{7-}$			2.5				
$TmPPP_2^{7-}$		4.700					

We thank Drs. B. E. Chapman and G. F. King for assistance with the operation of the NMR spectrometers and stimulating discussions. We also thank B. T. Bulliman and W. G. Lowe for computing and expert technical assistance, respectively.

This work was supported by a grant from the Australian National Health and Medical Research Council. A. R. Waldeck acknowledges the support of a University of Sydney Postgraduate Research Award.

Received for publication 21 May 1992 and in final form 11 January 1993.

REFERENCES

1. Westerhoff, H. V., and K. van Dam. 1987. *In* Thermodynamics and Biological Free Energy Transduction. Elsevier (Biomedical Division), Amsterdam. 190–191.
2. Bennekou, P. 1988. Steady-state and transient membrane potentials in human red cells determined by protonophore-mediated pH changes. *J. Membr. Biol.* 106:41–46.
3. Hellingwerf, K. J., J. C. Arents, B. J. Schulte, and H. V. Westerhoff. 1979. Bacteriorhodopsin in liposomes. II. Experimental evidence in support of a theoretical model. *Biochim. Biophys. Acta.* 547:561–582.
4. Van Walraven, H. S., H. J. P. Marvin, E. Koppenaal, and R. Kraayenhof. 1984. Proton movements and electric potential generation in reconstituted ATPase proteolipsomes from the cyanobacterium *Synechococcus* 6716. *Eur. J. Biochem.* 144:555–561.
5. Sarkadi, B., J. K. Alifimoff, R. B. Gunn, and D. C. Tosteson. 1978. Kinetics and stoichiometry of Na-dependent Li transport in human red blood cells. *J. Gen. Physiol.* 72:249–265.
6. McLaughlin, S. 1989. The electrostatic properties of membranes. *Annu. Rev. Biophys. Biophys. Chem.* 18:113–136.
7. Barry, P. H., and J. M. Diamond. 1984. Effects of unstirred layers on membrane phenomena. *Physiol. Rev.* 64:763–871.
8. Patey, G. N., and G. M. Torrie. 1989. Water and salt water near charged surfaces: a discussion of some recent theoretical results. *Chem. Scripta.* 29A:39–47.
9. Läuger, P., W. Lesslauer, E. Marti, and J. Richter. 1967. Electrical properties of bimolecular phospholipid membranes. *Biochim. Biophys. Acta.* 135:20–32.
10. Kamp, F., Y. Chen, and H. V. Westerhoff. 1988. Energization redistribution of charge carriers near membranes. *Biophys. Chem.* 30:113–132.
11. Tanford, C. 1961. *In* Physical Chemistry of Macromolecules. John Wiley and Sons, New York. 225–227.
12. Läuger, P. 1991. *In* Electrogenic ion Pumps. Sinnauer Associates, Sunderland, MA. 100–103.
13. Raftos, J. E., B. T. Bulliman, and P. W. Kuchel. 1990. Evaluation of an electrochemical model of erythrocyte pH buffering using ^{31}P nuclear magnetic resonance. *J. Gen. Physiol.* 95:1183–1204.
14. Kuchel, P. W. 1990. Spin-exchange NMR spectroscopy in studies of the kinetics of enzymes and membrane transport. *NMR Biomed.* 3:102–119.
15. Kuchel, P. W., B. T. Bulliman, B. E. Chapman, and K. Kirk. 1987. The use of transmembrane differences in saturation transfer for measuring fast membrane transport; application to $H^{13}CO_3^-$ exchange across the human erythrocyte. *J. Magn. Reson.* 74:1–11.
16. Potts, J. R., A. M. Hounslow, and P. W. Kuchel. 1990. Exchange of fluorinated glucose across the red-cell membrane measured by ^{19}F-n.m.r. magnetization-transfer. *Biochem. J.* 266:925–928.
17. Potts, J. R., and P. W. Kuchel. 1991. Anomeric preference of fluoro-glucose exchange across human red cell membranes: ^{19}F-n.m.r. studies. *Biochem. J.* 281:753–759.
18. Riddell, F. G., and S. Arumugam. 1989. The transport of Li^+, Na^+ and K^+ ions through phospholipid bilayers by the antibiotic M139603 studied by ^7Li-, ^{23}Na-, and ^{39}K-NMR. *Biochim. Biophys. Acta.* 984:6–10.
19. Shungu, D. C., and R. W. Briggs. 1988. Application of 1D and 2D ^{23}Na magnetization-transfer NMR to the study of ionophore-mediated transmembrane cation transport. *J. Magn. Reson.* 77:491–503.
20. Shungu, D. C., D. C. Buster, and R. W. Briggs. 1990. ^{23}Na Magnetization-transfer NMR studies of concentration and temperature dependence of ionophore-induced equilibrium exchange of Na^+ across prototypical cell membranes. *J. Magn. Reson.* 89:102–122.
21. Buster, D. C., J. F. Hinton, F. S. Millet, and D. C. Shungu. 1988. ^{23}Na-Nuclear magnetic resonance investigation of gramicidin-induced ion transport through membranes under equilibrium conditions. *Biophys. J.* 53:142–152.
22. Easton, P. L., J. F. Hinton, and D. K. Newkirk. 1990. Kinetics of the channel formation of gramicidins A and B in phospholipid vesicle membranes. *Biophys. J.* 57:63–69.
23. Gupta, R. J., and P. Gupta. 1982. Direct observation of resolved resonances from intra- and extracellular sodium-23 ions in NMR studies of intact cells and tissues using dysprosium (III)tripolyphosphate as a paramagnetic shift reagent. *J. Magn. Reson.* 47:344–350.
24. Chu, S. C., M. M. Pike, E. T. Fossel, T. W. Smith, J. A. Balshi, and C. S. Springer. 1984. Aqueous shift reagents for high-resolution cationic nuclear magnetic resonance. III. $Dy(TTHA)^{3-}$, $Tm(TTHA)^{3-}$, and $Tm(PPP)_2^{7-}$. *J. Magn. Reson.* 56:33–47.
25. Perrin, C. L., and R. K. Gipe. 1984. Multisite kinetics by quantitative two-dimensional NMR. *J. Am. Chem. Soc.* 106:4036–4038.
26. Jeener, J., B. A. Meier, P. Bachmann, and R. R. Ernst. 1979. Investigation of exchange processes by two-dimensional NMR spectroscopy. *J. Chem. Phys.* 71:4546–4553.
27. Kuchel, P. W., B. T. Bulliman, B. E. Chapman, and G. L. Mendz.

1988. Variances of rate constants estimated from 2D NMR exchange spectra. *J. Magn. Reson.* 76:136–142.

28. Chapman, B. E., I. M. Stewart, B. T. Bulliman, G. L. Mendz, and P. W. Kuchel. 1988. ^{31}P magnetization-transfer in the phosphoglyceromutase-enolase coupled enzyme system. *Eur. Biophys. J.* 16:187–191.
29. Bulliman, B. T., P. W. Kuchel, and B. E. Chapman. 1989. "Overdetermined" one-dimensional NMR exchange analysis. A 1D counterpart of the 2D EXSY experiment. *J. Magn. Reson.* 82:131–138.
30. Szoka, F., and D. Papahadjopoulos. 1978. Procedure for preparation of liposomes with large internal aqueous space and high capture by reverse phase evaporation. *Proc. Natl. Acad. Sci. USA.* 75:4194–4198.
31. New, R. R. C. 1990. *In* Liposomes: A Practical Approach. Oxford University Press, New York. 72–74.
32. Levitt, M. H., and R. R. Ernst. 1983. Composite pulses constructed by a recursive expansion procedure. *J. Magn. Reson.* 55:247–254.
33. Osborne, M. R. 1976. Non-linear least-squares regression; the Levenberg algorithm revisited. *J. Aust. Math. Soc.* B19:343–357.
34. Wolfram, S. 1991. *In* Mathematica. 2nd ed. Addison-Wesley, Redwood City, CA. 692–695.
35. Riddell, F. G., and S. Arumugam. 1988. Surface charge effects upon membrane transport processes: the effects of surface charge on the monensin-mediated transport of lithium ions through phospholipid bilayers studied by ^{7}Li-NMR spectroscopy. *Biochim. Biophys. Acta.* 945:65–72.
36. Brown, F. F. 1983. The effect of compartmental location on the proton T_2^* of small molecules in cell suspensions: a cellular field gradient model. *J. Magn. Reson.* 54:385–399.
37. Kuchel, P. W., and B. T. Bulliman. 1989. Perturbation of homogeneous magnetic fields by isolated single and confocal spheroids. Implications for NMR spectroscopy of cells. *NMR Biomed.* 2:151–159.
38. Roux, M., and J.-M. Neumann. 1986. Deuterium NMR study of headgroup deuterated phosphatidylserine in pure and binary phospholipid bilayers. *FEBS Lett.* 199:33–38.
39. Hope, M. J., M. B. Bally, L. D. Mayer, A. S. Janoff, and P. R. Cullis. 1986. Generation of multilamellar and unilamellar phospholipid vesicles. *Chem. Phys. Lipids.* 40:89–107.
40. McLaughlin, A., C. Grathwohl, and S. McLaughlin. 1978. The adsorption of divalent cations to phosphatidylcholine membranes. *Biochim. Biophys. Acta.* 513:338–357.
41. Lieber, M. R., and T. L. Steck. 1982. Dynamics of the holes in human erythrocyte membrane ghosts. *J. Biol. Chem.* 257: 11660–11666.
42. Shedd, S. F., and L. D. Spicer. 1991. Characterization of a microcarrier cell culture system for ^{23}Na MR spectroscopy studies. *NMR Biomed.* 4:246–253.
43. Furó, I., B. Halle, P.-O. Quist, and T. C. Wong. 1990. Counterion surface diffusion in a lyotropic mesophase. A ^{23}Na two-dimensional quadrupolar echo relaxation study. *J. Phys. Chem.* 94:2600–2613.
44. Tiddy, G. J. T. 1977. Nuclear magnetic resonance studies of liquid crystal phase structure and self-diffusion coefficients in the system lithium perfluoro-octanoate+water. *J. Chem. Soc. Faraday Trans. I* 73:1733–1737.